Quantum properties of nitrogen-vacancy center in diamond coupled to mechanical resonators

Qinghong Liao[1,2,3], Min Xiao[1], Haiyan Qiu[1] and Menglin Song[1]

[1] Department of Electronic Information Engineering, Nanchang University, Nanchang 330031, China;
[2] State Key Laboratory of Low-Dimensional Quantum Physics, Department of Physics, Tsinghua University, Beijing 100084, China

[3] Corresponding author's email: nculqh@163.com

Abstract. The optical absorption spectrum of the hybrid system composed of the nitrogen-vacancy (NV) center coupled to the mechanical resonators is. investigated. Based on the pump-probe technology, the electronically induced transparency (EIT) is observed and the reasonable explanation for this transparency is given. We demonstrate that the position of the transparency is equal to the detuning difference. In addition, a completely new scheme to measure the coupling between the NV center and current carrying carbon nanotube mechanical resonator is obtained. Furthermore, an optical approach to measure the frequency of the vibrating graphene mechanical resonator is proposed. This work can provide some help for the application in the field of high-precision measurement and quantum information processing.

1. Introduction

The NV centers in diamond are promising materials, which has applications in quantum information processing [1-3] and nanoscale field sensors [4]. Due to some excellent properties of NV center, such as long coherence times [5,6] and high controllability [6-11], it can couple with many sorts of external fields and combine two or more kinds of physical systems to form a hybrid quantum system. For example, it has been coupled with photons [12,13], nuclear spin [6,14], magnetic field and mechanical resonator [15-21] through scientific experiments.

The research of nanomechanical systems, such as current carrying carbon nanotubes [22] and vibrating graphene mechanical resonators, is currently receiving much attention. They have some applications in like quantum information processing [18, 20-23], quantum measurements [23-25] and force detection [26,27]. Many efforts have been made to study on the hybrid spin-NR system. A magnetic coupling between the nanomechanical resonator and the NV electronic spin can be induced in a strong magnetic field gradient[28]. This hybrid system, which is composed of NV center and resonator, is susceptible to reach the strong coupling regime, as already envisioned in ref. [29,30]. Li et al. have proposed a hybrid system in which a single NV center spin in diamond is coupled to a suspended current-carrying carbon nanotube[31]. The strong coupling mechanism and coherent manipulation in this hybrid quantum has been realized, which establishes a theoretical foundation for us to study further. Moreover, the optomechanical system based on graphene resonator has also been investigated experimentally [32-35].

Weber et al. proposed a scheme of coupling graphene resonators with superconducting cavities, which can significantly reduce the resonant frequency of graphene resonators, thus enhancing zero

motion and increasing mechanical nonlinearity, which has important prospects for the study of quantum motion[33].

In this work, motivated by these developments, we propose a hybrid system consisting of nitrogen-vacancy center in diamond coupled to mechanical resonators. The presented work has some remarkable advantages. Firstly, the EIT has been observed in both diamond NV center coupled to a single graphene resonator or a single carbon nanotube resonator, as well as in both graphene and carbon nanotube resonator. Moreover, the position of EIT can be tuned by controlling the detuning between the NV center and current carrying carbon nanotube resonator. Secondly, an optical method is proposed to measure coupling strength and the frequency of resonator.

The structure of this paper is organized as follows. In the second section, the physical model and the basic numerical calculation for the present system are given. The EIT is observed and the reason for it is given in the third section. Besides, the schemes to measure the coupling strength between the NV center and current carrying carbon nanotube mechanical resonator and the frequency of vibrating graphene mechanical resonator are obtained. Finally, a conclusion is given in the fourth section.

2. Physical model and calculations

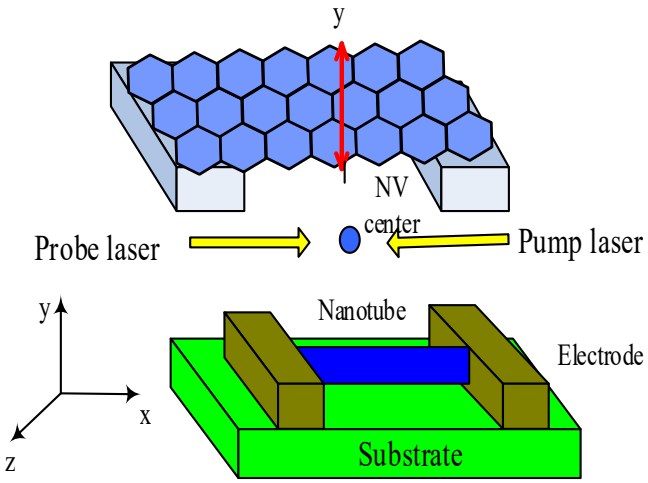

Figure 1. The Physical model of this system.

The hybrid system is presented in Figure 1, which is composed of NV center in diamond, vibrating graphene resonator and a current carrying carbon nanotube resonator. The system is driven by pump and probe field simultaneously. The graphene membrane is laid in the x-z plane and vibrates along the y-direction in the system [36]. The Hamiltonian of the NV center in diamond can be characterized by the pseudospin -1/2 operators $S^{\pm}$ and S^{z}. So its Hamiltonian can be described by $H_{NV}=\hbar\omega_{ex}S^{z}$ [37], where ω_{ex} is the frequency of the NV center. The Hamiltonian of the vibrating graphene membrane is $H_{vgm}=\hbar\omega_1 a_1^{\dagger}a_1$ [38], where ω_1 means the frequency of the vibrating graphene membrane and $a_1\left(a_1^{\dagger}\right)$ is the annihilation (creation) operator for the vibrating graphene membrane. The Hamiltonian of the current carrying carbon nanotube can be written as $H_{cnt}=\hbar\omega_2 a_2^{\dagger}a_2$, where ω_2 denotes the frequency of the current carrying carbon nanotube and $a_2\left(a_2^{\dagger}\right)$ describes the annihilation (creation) operator for the current carrying carbon nanotube. The interaction Hamiltonian between the NV center and the vibrating graphene membrane is $H_{NV-vgm}=\hbar\lambda_1 S^{z}\left(a_1^{\dagger}+a_1\right)$ [17]. And $H_{NV-cnt}=\hbar\lambda_2\left(S^{+}a_2+S^{-}a_2^{\dagger}\right)$ [29,39] means the interaction Hamiltonian between the NV center and the current carrying carbon nanotube. The coupling strength between the NV center and the vibrating graphene membrane (current carrying

nanotube) is $\lambda_1(\lambda_2)$. The Hamiltonian of the NV center coupled to the pump laser and probe laser is given by $H=-\mu\left(S^+E_{pu}e^{-i\omega_{pu}t}+S^-E_{pu}^*e^{i\omega_{pu}t}\right)-\mu\left(S^+E_{pr}e^{-i\omega_{pr}t}+S^-E_{pr}^*e^{i\omega_{pr}t}\right)$, where μ is the dipole moment; $\omega_{pu}(\omega_{pr})$ denotes the frequency of the pump field (probe field); $E_{pu}\left(E_{pr}\right)$ means the amplitude of the pump field (probe field).

So the Hamiltonian of the system is read as follows ($\hbar=1$):

$$\begin{aligned}H=&\omega_1a_1^\dagger a_1+\omega_2a_2^\dagger a_2+\omega_{ex}S^z+\lambda_1S^z\left(a_1^\dagger+a_1\right)+\lambda_2\left(S^+a_2+S^-a_2^\dagger\right)\\&-\mu\left(S^+E_{pu}e^{-i\omega_{pu}t}+S^-E_{pu}^*e^{i\omega_{pu}t}\right)-\mu\left(S^+E_{pr}e^{-i\omega_{pr}t}+S^-E_{pr}^*e^{i\omega_{pr}t}\right).\end{aligned}\tag{1}$$

In the rotating frame at the pump field frequency ω_{pu}, the Hamiltonian can be rewritten as

$$\begin{aligned}H=&\omega_1a_1^\dagger a_1+\Delta_ca_2^\dagger a_2+\Delta_{pu}S^z+\lambda_1S^z\left(a_1^\dagger+a_1\right)+\lambda_2(S^+a_2-S^-a_2^?)\\&-\Omega_{pu}(S^+-S^-)-\mu E_{pr}(S^+\,\mathrm{e}^{-i\delta t}-S^-\,\mathrm{e}^{i\delta t}),\end{aligned}\tag{2}$$

where $\Delta_c=\omega_2-\omega_{pu}$ is the detuning between the current carrying carbon and pump field, $\Delta_{pu}=\omega_{ex}-\omega_{pu}$ means the detuning between NV center and pump field, $\Omega_{pu}=\mu E_{pu}/\hbar$ represents Rabi frequency of pump field, and $\delta=\omega_{pr}-\omega_{pu}$ stands for the detuning of the frequency of the probe field and the pump field.

The Heisenberg-Langevin equations can be easily obtained as follows. Here quantum properties of S^z, S^- and N is ignored, and introduce the damping and noise terms.

$$\begin{aligned}&\frac{dS^z}{dt}=-\Gamma_1(S^z+1/2)-i\lambda_2\left(S^+a_2-S^-a_2^+\right)\\&+i\Omega_{pu}(S^+-S^-)+\frac{i\mu E_{pr}}{\hbar}(S^+\,\mathrm{e}^{-i\delta t}-S^-\,\mathrm{e}^{i\delta t}),\end{aligned}\tag{3}$$

$$\begin{aligned}&\frac{dS^-}{dt}=\left[-i\left(\Delta_{pu}+\lambda_1N\right)+\Gamma_2\right]S^-+2i\lambda_2a_2S^z\\&-2i\Omega S^z-2\frac{i\mu E_{pr}}{\hbar}e^{-i\delta t}S^z+f(t),\end{aligned}\tag{4}$$

$$\frac{da_2}{dt}=-\left(i\Delta_c+\kappa_m/2\right)a_2-i\lambda_2S^-+\xi(t),\tag{5}$$

$$\frac{d^2N}{dt^2}+\gamma_n\frac{dN}{dt}+\omega_1^2N=-2\omega_1\lambda_1S^z+\xi(t),\tag{6}$$

where $N=a_1+a_1^\dagger$ denotes the position operator; the Γ_1 and Γ_2 represent the relaxation rate and dephasing rate of the NV center, respectively. The κ_m and γ_n are the damping rate of the current carrying carbon nanotube and the vibrating graphene membrane, respectively. $\xi(t)$ is quantum Brownian stochastic noise, which has zero mean value. Its correlation function is

$$\left\langle\xi^\dagger(t)\xi(t)\right\rangle=\frac{\gamma_m}{\omega_m}\int\frac{d\omega}{2\pi}\omega e^{-i\omega(t-t')}\left[1+\coth\left(\frac{\hbar\omega}{2\kappa_BT}\right)\right],\tag{7}$$

where κ_B and T indicate the Boltzmann constant and the temperature of the reservoir of the coupled system, respectively. $\tau(t)$ means the Langevin noise operators in the system with zero mean value $\left\langle f(t)\right\rangle$=0 and follows correlation functions $\left\langle f^\dagger(t)f(t)\right\rangle$ □ $\delta(t-t')$.

To solve Eqs. (3)-(6), we make the ansatz.:

$$S^z(t)=S_0^z+S_+^ze^{-i\delta t}+S_-^ze^{i\delta t},\tag{8}$$

$$S^-(t)=S_0+S_+e^{-i\delta t}+S_-e^{i\delta t},\tag{9}$$

$$N(t) = N_0 + N_+ e^{-i\delta t} + N_- e^{i\delta t}, \tag{10}$$

$$a_2(t) = a_2 + a_{2+} e^{-i\delta t} + a_{2-} e^{i\delta t}. \tag{11}$$

Then the steady-state solutions are obtained as follows:

$$N_0 = \frac{-2\lambda_1 S_0^z}{\omega_1}, \tag{12}$$

$$a_2 = \frac{-i\lambda_2 S_0}{\gamma}, \tag{13}$$

$$S_0 = \frac{-\omega_0 \Omega_{pu} i}{d_2 - d_1 \omega_0}, \tag{14}$$

where $\gamma = (i\Delta_c + \kappa_m/2)$, $d_2 = i\Delta_{pu} + \Gamma_2$, $d_1 = i\frac{\lambda_1^2}{\omega_1} + \frac{\lambda_2^2}{\gamma}$.

The above steady-state solutions N_0, a_2 and S_0, have a connection with the population inversion $(\omega_0 = 2S_0^z)$ of the NV center, which is determined by

$$\begin{aligned} &\Gamma_1(\omega_0 + 1)\gamma\gamma^*\left(\kappa_m^2/4 + \Delta_c^2\right)\left(d_2^* - d_1^*\omega_0\right)\left(d_2 - d_1\omega_0\right) \\ &+4\gamma\gamma^*\Omega_{pu}^2\omega_0 + \Gamma_2\left(\kappa_m^2/4 + \Delta_c^2\right) - 2\Omega_{pu}^2\omega_0\gamma\gamma^* k_m\omega_0\lambda_2^2 \\ &+4i\lambda_2^2\Omega_{pu}^2\omega_0^2\Delta_c\left(\kappa_m^2/4 + \Delta_c^2\right) = 0. \end{aligned} \tag{15}$$

Bringing the Eqs. (9)-(12) into Eqs. (3)-(6), the linear optical susceptibility is obtained as $\chi^{(1)}(\omega_{pr}) = \mu S_+ / E_{pr} = \mu^2 / \Gamma_2 \hbar \chi(\omega_{pr})$ and $\chi(\omega_{pr})$ is given by

$$\chi(\omega_{pr}) = \frac{\alpha_1\theta_3\left(\alpha_3^*\theta_1 + \alpha_4^*\right) - i\omega_0\alpha_4^*}{\alpha_2\alpha_4^* - \alpha_1\alpha_3^*\theta_1\theta_4^*}, \tag{16}$$

where $\beta_1 = \frac{-i\lambda_2}{i\Delta_c + \kappa_m/2 - i\delta}$, $\beta_2 = \frac{-i\lambda_2}{i\Delta_c + \kappa_m/2 + i\delta}$, $\eta = \frac{2\omega_1\lambda_1}{\delta^2 + i\delta\gamma_n - \omega_1^2}$, $\theta_1 = \frac{i\Omega_{pu} - i\lambda_2 S_0\beta_2^* + i\lambda_2 a_2}{\Gamma_1 - i\delta}$,

$\theta_2 = \frac{-i\Omega_{pu} + i\lambda_2 S_0^*\beta_1 - i\lambda_2 a_2^*}{\Gamma_1 - i\delta}$, $\theta_3 = \frac{iS_0^*}{\Gamma_1 - i\delta}$, $\alpha_1 = -i\lambda_1 S_0\eta + 2i\lambda_2 a_2 - 2i\Omega_{pu}$,

$\alpha_2 = i\Delta_{pu} + \Gamma_2 + i\lambda_1 N_0 - i\delta - i\lambda_2\beta_1\omega_0 - \alpha_1\theta_2$, $\alpha_3 = -i\lambda_1 S_0\eta^* + 2i\lambda_2 a_2 - 2i\Omega_{pu}$,

$\alpha_4 = i\Delta_{pu} + \Gamma_2 + i\lambda_1 N_0 + i\delta - i\lambda_2\beta_2\omega_0 - \alpha_3\theta_1^*$.

(O^* denotes the conjugate of O)

3. Results and discussions

In order to study the phenomenon of EIT comprehensively, we depict the absorption spectrum as a function of Δ_{pr} in Figure 2. The black curve denotes the probe absorption spectrum without any couplings in Figure 2(a). It has the characteristics of symmetry and complete absorption. Figure 2(b) plots the probe absorption spectrum with the coupling between the NV center and the current carrying carbon nanotube, which has a zero absorption at the position of $\Delta_{pr} = 0$. This shows that the phenomenon of EIT occurs. The probe absorption spectrum in the present of the coupling between the NV center and graphene membrane is plotted in Figure 2(c). It presents two points that have a zero absorption because of the mechanically induced three-photon resonance [40]. The probe absorption spectrum of the NV center simultaneously coupled to the current carrying carbon nanotube and vibrating graphene membrane is shown in Figure 2(d). There are three positions that the absorption is zero. Moreover, the positions are same with the Figure 2(b) and Figure 2(c), respectively. We can note that the height of the peaks is raised compared with Figure 2(c). It is due to the fact that the interaction between NV center and the vibrating graphene membrane strengthens the EIT phenomenon.

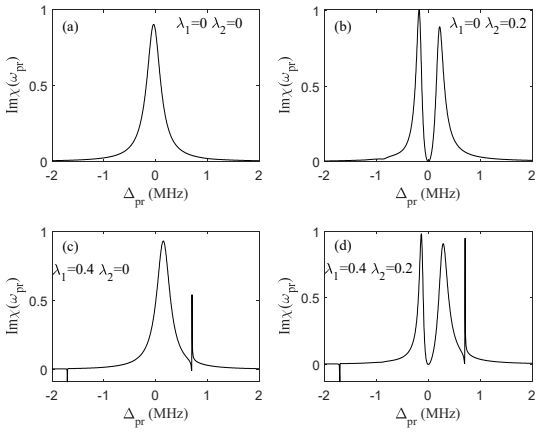

Figure 2. (a) The absorption spectrum as a function of Δ_{pr} without any couplings. (b) with the coupling $\lambda_2 = 0.2$. (c) with the coupling $\lambda_1 = 0.4$. (d) with the coupling $\lambda_1 = 0.4$ and $\lambda_2 = 0.2$. The other parameters are Γ_1=0.3MHz, Γ_2=0.15MHz, ω_1=1.2MHz, $\Delta_{pu} = 0.5$MHz, $\Delta_c = 0.5$ MHz and $\Omega_{pu}^2 = 0.01(\text{MHz})^2$.

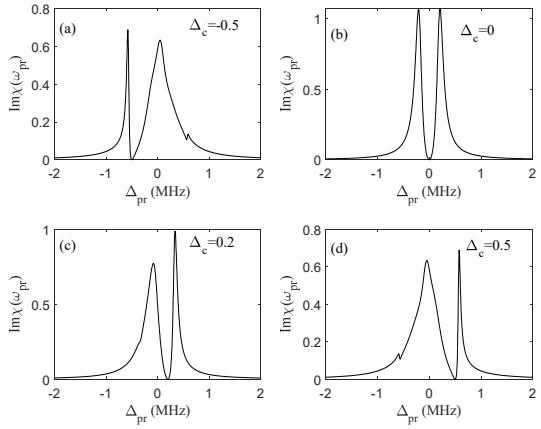

Figure 3. (a), (b), (c) and (d) denote the absorption spectrum as a function of Δ_{pr} with the detuning of the NV center and the current carrying carbon nanotube is -0.5, 0, 0.2, 0.5, respectively. Other parameters are same with Figure 2 besides $\Delta_{pu} = 0$.

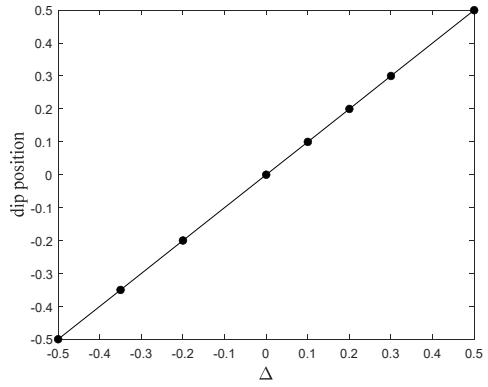

Figure 4. The relationship between the dip position and the value of Δ. The parameters are same with Figure 3.

As illustrated in Figure 3, the location of the window of EIT at different values of detuning of NV center and the current carrying carbon nanotube is depicted. Figure 3(a) denotes that when the detuning of the NV center and the current carrying carbon nanotube (Δ_c) is -0.5, the EIT window occurs at the value of $\Delta_{pr} = -0.5$. The dip locates at zero while the $\Delta_c = 0$ shown in Figure 3(b). And if the detuning value is $\Delta_c = 0.2$, there will be a dip at $\Delta_{pr} = 0.2$ as shown in Figure 3(c). The Figure 3(d) gives the similar result, which has a zero absorption at $\Delta_{pr} = 0.5$ as the detuning value is 0.5. Therefore, we can obtain a result that the location of EIT window is equal to the value of $\Delta_c - \Delta_{pu}$. Here, we set the Δ is equal to $\Delta_c - \Delta_{pu}$. This ascribes to the reason that the mechanically induced coherent population oscillation leads to the occurring transparency window. To verify this result, we draw a diagram of the relationship between the position of dip and the value of Δ in Figure 4. From this figure, a linear relationship between the position of dip and the value of Δ is obtained. Undoubtedly, it is known the information that the location of EIT window is equal to the value of Δ.

Figure 5 shows the absorption spectrum as a function of Δ_{pr} with or without the coupling between diamond NV center and current carrying carbon nanotube. It demonstrates the coupling strength can be obtained by measuring the distance of the peak-splitting. There is only an absorption peak (black solid line) under the condition of the coupling between diamond NV center and current carrying carbon nanotube is zero. But when the coupling is added, the absorption spectrum splits into two peaks and has a zero absorption point at $\Delta_{pr} = 0$. And as the coupling strength becomes larger and larger, the width of transparency window is wider and wider. The physical mechanism of this result is due to the mechanically induced coherent population oscillation. When the detuning of the detection pump is equal to the frequency of the resonator, it makes the diamond NV center interfere with the beat frequency of the two light fields [41]. The splitting distance of two peaks as a function of the coupling strength is shown in the inset of Figure 5. It is found that the splitting distance is linear with the coupling strength. Consequently, the result provides an effective method to measure the coupling strength between diamond NV center and current carrying carbon nanotube. Therefore, a method is proposed to obtain the coupling strength only by measuring the distance of two peaks in the probe absorption spectrum.

The absorption spectrum as a function of Δ_{pr} for three different frequencies of the vibrating graphene membrane is shown in Figure 6. It is noted that there exist two peaks, a right positive peak and a left negative peak, whatever the frequency is. The two peaks correspond to the resonant absorption and amplification of the mechanical mode, respectively. Besides, the position of the peak is exactly equal to the frequency of the vibrating graphene membrane. Therefore, a new approach to measure the frequency of the vibrating graphene membrane is provided. It is mainly divided into two steps. Firstly, the frequency of the first pump light should be fixed at the frequency of the NV center, and then the second probe light should be swept across the frequency range of the NV center. It is found that there exist two sharp peaks in the absorption spectrum of the probe light, and the positions of the peaks correspond to the vibration frequency of the vibrating graphene membrane. The basic principle of this method is mechanically induced coherent population oscillation. What's more, with the frequency of vibrating graphene membrane becomes larger and larger, the width of EIT window at $\Delta_{pr} = -0.5$ turns narrower and narrower. The reason for this result is that the quantum coherent interaction between NV center and vibrating graphene membrane.

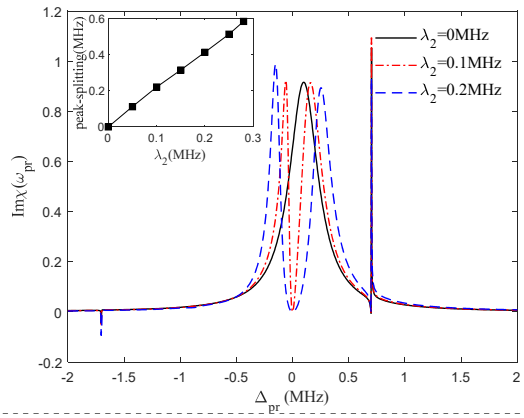

Figure 5. The absorption spectrum as a function of Δ_{pr} for three different coupling strengths between diamond NV center and current carrying carbon nanotube. The inset is the splitting distance of two peaks as a function of the coupling strength. The different parameter used is λ_1=0.3 and other parameters are same with Figure 2.

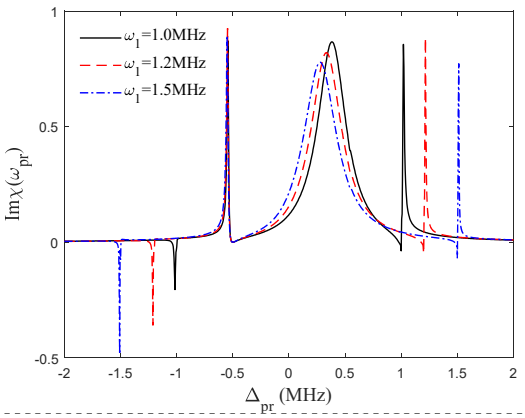

Figure 6. The absorption spectrum as a function of Δ_{pr} for three different frequencies of the vibrating graphene membrane. The parameters are Γ_1=0.3MHz, Γ_2=0.15MHz, $\Delta_{pu}=0$, $\Delta_c=-0.5$MHz, $\Omega_{pu}^2=0.01(\text{MHz})^2$, λ_1=0.6MHz and λ_2=0.2MHz.

4. Conclusion

In summary, we have proposed a hybrid system based on the NV center and mechanical resonators. We have found that there is a zero absorption in the absorption spectrum when the NV center couples either the vibrating graphene membrane or the current carrying carbon nanotube. It indicates that the phenomenon of the EIT occurs at that position. Additionly, the relationship between the position of EIT window and the value of detuning difference have been demonstrated. Moreover, an approach to measure the frequency of vibrating graphene membrane is obtained. Our works may have potential applications on the quantum precision measurement.

Acknowledgements

This project was supported by the National Natural Science Foundation of China (Grant No. 62061028), the Opening Project of Shanghai Key Laboratory of Special Artificial Microstructure Materials and Technology(Grant No. ammt2021A-4), the Foundation for Distinguished Young Scientists of Jiangxi Province (Grant No. 20162BCB23009), the Open Research Fund Program of the State Key Laboratory of Low-Dimensional Quantum Physics (Grant No. KF202010), the Interdisciplinary Innovation Fund of Nanchang University (Grant No. 9166-27060003-YB12), and the Open Research Fund Program of Key Laboratory of Opto-Electronic Information Acquisition and Manipulation of Ministry of Education (Grant No. OEIAM202004)

References

[1] C. Monroe 2002 Quantum information processing with atoms and photons *Nature* **416** 238
[2] Z. L. Xiang, S. Ashhab, J. Q. You, F. Nori 2013 Hybrid quantum circuits: Superconducting circuits interacting with other quantum systems *Rev. Mod. Phys.* **85** 623
[3] G. Kurizki, P. Bertet, Y. Kubo, K. Mølmer, D. Petrosyan, P. Rabl, J. Schmiedmayer 2015 Quantum technologies with hybrid systems *Proc. Natl. Acad. Sci.* **112** 3866
[4] L. Childress, M. V. G. Dutt, J. M. Taylor, A. S. Zibrov, F. Jelrzko, J. Wrachtrup, P.R. Hemmer, M.D. Lukin 2006 Coherent dynamics of coupled electron and nuclear spin qubits in diamond *Science* **314** 281

[5] N. Bar-Gill, L. M. Pham, A. Jarmola, D. Budker, R. L. Walsworth 2013 Solid-state electronic spin coherence time approaching one second *Nat. Commun.* **4** 1
[6] S. Hong, M. S. Grinolds, P. Maletinsky, R. L. Walsworth, M. D. Lukin, A. Yacoby 2012 Coherent, mechanical control of a single electronic spin *Nano Lett.* **12** 3920
[7] R. Hanson, D. D. Awschalom 2008 Coherent manipulation of single spins in semiconductors *Nature* **453** 1043
[8] T. Gaebel, M. Domhan, I. Popa, C. Wittmann, P. Neumann, F. Jelezko, J. R. Rabeau, N. Stavrias, A. D. Greentree, S. Prawer, J. Meijer, J. Twamley, P. R. Hemmer, J. Wrachtrup 2006 Room-temperature coherent coupling of single spins in diamond *Nat. Phys.* **2** 408
[9] M.W. Doherty, N.B. Manson, P. Delaney, F. Jelezko, J. Wrachtrup, L.C. Hollenberg 2013 The nitrogen-vacancy colour centre in diamond *Phys. Rep.* **528** 1
[10] R. Hanson, F. M. Mendoza, R. J. Epstein, D. D. Awschalom 2006 Polarization and readout of coupled single spins in diamond *Phys. Rev. Lett.* **97** 087601
[11] E. Togan, Y. Chu, A. S. Trifonov, L. Jiang, J. Maze, L. Childress, M.V.G. Dutt, A.S. Sørensen, P.R. Hemmer, A.S. Zibrov, M.D. Lukin 2010 Quantum entanglement between an optical photon and a solid-state spin qubit *Nature* **466** 730
[12] H. Bernien, B. Hensen, W. Pfaff, G. Koolstra, M. S. Blok, L. Robledo, T.H. Taminiau, M. Markham, D.J. Twitchen, L. Childress, R. Hanson 2013 Heralded entanglement between solid-state qubits separated by three metres *Nature* **497** 86
[13] A. Faraon, P. E. Barclay, C. Santori, K. M. C. Fu, R. G. Beausoleil 2011 Faraon A, Barclay P E, Santori C, et al. Resonant enhancement of the zero-phonon emission from a colour centre in a diamond cavity *Nat. Photon.* **5** 301
[14] H. S. Knowles, D. M. Kara, M. Atatüre 2017 Controlling a nuclear spin in a nanodiamond *Phys. Rev. B* **96** 115206
[15] S. Kolkowitz, A. C. B. Jayich, Q. P. Unterreithmeier, S. D. Bennett, P. Rabl, J. G. E. Harris, M.D. Lukin 2012 Coherent sensing of a mechanical resonator with a single-spin qubit *Science* **335** 1603
[16] A. Chowdhury, P. Vezio, M. Bonaldi, A. Borrielli, F. Marino, B. Morana, G. A. Prodi, P. M. Sarro, E. Serra, F. Marin 2020 Quantum signature of a squeezed mechanical oscillator *Phys. Rev. Lett.* **124** 023601
[17] P. Rabl, P. Cappellaro, M. G. Dutt, L. Jiang, J. R. Maze, M. D. Lukin 2009 Strong magnetic coupling between an electronic spin qubit and a mechanical resonator *Phys. Rev. B* **79** 041302
[18] S. Rips, M. J. Hartmann 2013 Quantum information processing with nanomechanical qubits *Phys. Rev. Lett.* **110** 120503
[19] J. Teissier, A. Barfuss, P. Appel, E. Neu, P. Maletinsky 2014 Strain coupling of a nitrogen-vacancy center spin to a diamond mechanical oscillator *Phys. Rev. Lett.* **113** 020503
[20] P. Ovartchaiyapong, K. W. Lee, B. A. Myers, A. C. B. Jayich 2014 The Brassica oleracea genome reveals the asymmetrical evolution of polyploid genomes *Nat. Commun.* **5** 1-14
[21] H. Jayakumar, B. Khanaliloo, D.P. Lake, P.E. Barclay 2014 Tunable amplification and cooling of a diamond resonator with a microscope *Phys. Rev. Appl.* **16** 014063
[22] B. L. Wang, B. Li, X. X. Li, F. L. Li, P. B. Li 2020 Generation of multiparticle entangled states of nitrogen-vacancy centers with carbon nanotubes[J] *Quantum Inf. Process.* **19** 1-19
[23] H. Okamoto, A. Gourgout, C. Y. Chang, K. Onomitsu, I. Mahboob, E. Y. Chang, H. Yamaguchi 2013 Coherent phonon manipulation in coupled mechanical resonators *Nat. Phys.* **9** 480
[24] A. D. O'Connell, M. Hofheinz, M. Ansmann, C. Bialczak, M. Lenander, L. Erik, M. Neeley, D. Sank, H. Wang, M. Weides, W. J. John, M. Martinis, A. N. Cleland 2010 Quantum ground state and single-phonon control of a mechanical resonator *Nature* **464** 697-703
[25] A. H. Safavi-Naeini, J. Chan, J. T. Hill, T. P. M. Alegre, A. Krause, O, Painter 2012 Observation of quantum motion of a nanomechanical resonator *Phys. Rev. Lett* **108** 033602
[26] D. Rugar, R. Budakian, H. J. Mamin, B. W. Chui 2004 Single spin detection by magnetic

resonance force microscopy *Nature* **430** 329-332
[27] J. Moser, J. Güttinger, A. Eichler, M.J. Esplandiu, D. E. Liu, M. I. Dykman, A. Bachtold 2013 Ultrasensitive force detection with a nanotube mechanical resonator *Nat. Nanotechnol.* **8** 493-496
[28] O. Arcizet, V. Jacques, A. Siria, P. Poncharal, P. Vincent, and S. Seidelin 2011 A single nitrogen-vacancy defect coupled to a nanomechanical oscillator *Nat. Phys.* **7** 879
[29] P. Rabl, P. Cappellaro, M. V. Gurudev Dutt, L. Jiang, J. R. Maze, and M. D. Lukin 2009 *Phys. Rev. B* **79** 041302
[30] P. Rabl, S. J. Kolkowitz, F. H. L. Koppens, J. G. E. Harris, P. Zoller, and M. D. Lukin 2010 *Nat. Phys.* **6** 602
[31] P. B. Li, Z. L. Xiang, P. Rabl, F. Nori 2016 Hybrid quantum device with nitrogen-vacancy centers in diamond coupled to carbon nanotubes *Phys. Rev. Letts.* **117** 015502
[32] R.A. Barton, R. StorchI, V.P. Adiga, R. Sakakibara, B.R. Cipriany, B. Ilic, S.P. Wang, P. Ong, P.L. McEuen, J.M. Parpia, H.G. Craighead 2012 Photothermal self-oscillation and laser cooling of graphene optomechanical systems *Nano Lett.* **12** 4681-4689
[33] P. Weber, J. Guttinger, I. Tsioutsios, D.E. Chang, A. Bachtold 2014 Coupling graphene mechanical resonators to superconducting microwave cavities *Nano Lett.* **14** 2854-2860
[34] X. Song, M. Oksanen, J. Li, P. J. Hakonen, M. A. Sillanpää 2014 Graphene optomechanics realized at microwave frequencies *Phys. Rev. Lett.* **113** 027404
[35] V. Singh, S. J. Bosman, B. H. Schneider, Y. M. Blanter, A. Castellanos-Gomez, G. A. Steele 2014 Optomechanical coupling between a multilayer graphene mechanical resonator and a superconducting microwave cavity *Nat. Nanotechnol.* **9** 820-824
[36] Q. H. Liao, G. Q. He 2020 Maximal entanglement and switch squeezing with atom coupled to cavity field and graphene membrane *Quantum Inf. Process.* **19** 1-19
[37] H. J. Chen, K. D. Zhu 2015 All-optical scheme for detecting the possible Majorana signature based on QD and nanomechanical resonator systems *Science China: Physics, Mechanics & Astronomy* **58** 1-18
[38] P. Rabl, S. J. Kolkowitz, F. H. L. Koppens, J. G. E. Harris, P. Zoller, M. D. Lukin 2012 A quantum spin transducer based on nanoelectromechanical resonator arrays *Nat. Phys.* **6** 602-608
[39] W. Xiong, J. Chen, B. Fang, M. Wang, L. Ye, J. Q. You 2021 Strong tunable spin-spin interaction in a weakly coupled nitrogen vacancy spin-cavity electromechanical system *Phys. Rev. B* **103** 174106
[40] J. J. Li, K. D. Zhu 2009 A scheme for measuring vibrational frequency and coupling strength in a coupled nanomechanical resonator-quantum dot system *Appl. Phys. Lett.* **94** 063116
[41] J. J. Li, K. D. Zhu 2013 All-optical mass sensing with coupled mechanical resonator systems *Phys. Rep.* **525** 223-254, 201